TRANSPORT AND CONVERGENCE OF THE NORTH ATLANTIC DRIFT CURRENT COMPUTED FROM THE AVERAGE JANUARY PRESSURE DISTRIBUTION*

By

EDWARD M. BROOKS

According to Montgomery (1936, 1938), one of the important effects of the wind blowing over the sea surface is its production of positive and negative convergence in the drift current, which is essentially limited to a surface homogeneous layer usually less than 50 meters thick. This convergence results from the net transport of the drift current at right angles to the wind, the magnitude of the transport being such that the deflecting force acting on it exactly compensates the wind stress. Of course, this involves the assumption that the drift current has come to equilibrium with the wind. To avoid boundary conditions, this theory should be applied only to the open ocean, away from coast lines and in deep water.

The purpose of this paper was to find the extreme variations of the transport and convergence of the drift current in the North Atlantic Ocean for average atmospheric conditions. Computations for January were carried out and compared with the results of Montgomery's investigation for July (Montgomery, 1936). Then the transport and convergence of the drift for the other months were estimated qualitatively from Defant's monthly average atmospheric pressure charts (Defant, 1917).

Two methods were employed in getting the January results. The first, following that used by Montgomery (1936), was based on gradient winds deduced from the January pressure distribution given by Defant (1917); whereas the second used direct wind observations collected by the Koninklijk Nederlandsch Meteorologisch Instituut (1919). As the first method has been adequately treated by Montgomery, only the second will be discussed here.

The wind speeds, which were estimated in Beaufort numbers, were converted into meters per second by use of the international Beaufort scale (Perlewitz, 1935). The formula used for getting the magnitude of the transport from the wind speed was

$$T = \frac{\tau_0}{f} = \frac{\rho\gamma^2 W_0^2}{2\Omega \sin L}$$

(Rossby and Montgomery, 1936), where T was the magnitude of the transport; τ_0, the shearing stress between wind and water; f, the Coriolis param-

* Contribution No. 229 of the Woods Hole Oceanographic Institution.

eter; ρ, the density of the air; γ^2, a stress coefficient; W_0, the surface wind speed; Ω, the angular velocity of the earth's rotation; and L, the latitude. γ^2 was taken as 0.0025 to conform with the choice of $z_0 = 0.6$ cm., used in the computations from Defant's pressures.

The transport and convergence calculated by the wind observations method were on the average about 20% larger than those obtained by the pressure method. Although this difference might be more marked if it were not for the existence of some atmospheric stability tending to reduce the surface wind speed below its theoretical value for a homogeneous atmosphere, the order of magnitude of the discrepancy seems relatively insignificant in view of the uncertainty of the applicability of the theory behind either computation. A second difference of more interest is the greater irregularity of the transport vectors and convergence magnitudes obtained from the wind method. It is doubtful whether the irregularities in the average winds can be explained by such atmospheric features as fixed anticyclonic cells in the Azores "high" or a mean polar front at a certain distance off the American coast because the positions of such semi-permanent elements might be too variable. Both of the differences found must be largely due to the fact that Defant got pressure values by interpolation with smoothed isobars, whereas the Dutch institute tabulated all observations without regard for geographical continuity.

The January transport and convergence computed from the average pressures of Defant are presented in Table I and Figure 52. The resemblance of the January chart to the July chart is quite pronounced in regard to both the distribution of the transport vectors and the magnitudes of the convergence, largely due to the existence of prevailing westerly winds in the north portion and easterly trades in the south portion at both times of year. On the other hand, minor seasonal differences in drift current movement occur in connection with the difference in size and shape of the Azores "high," which is less circular and has a weaker central pressure in January than in July. The average January transport is generally larger than that of July, corresponding to greater strength of the Icelandic "low" and steeper pressure gradients in the trade-wind belt in January. Along the average high pressure belt convergence is smaller, and in the extreme south it is larger than in July. Also, negative convergence, or divergence, is more marked in the Newfoundland region in January, when the mean isobars have a definite cyclonic curvature.

Although Defant's monthly average pressure maps suggest that the January and July conditions stand at opposite extremes in the annual cycle of average pressure distribution, the changes from one month to the other are not strictly uniform, as indicated by the maps for intervening months. Consequently, the annual trend of the more important features of the drift current deserves analysis from the monthly maps, even though the total variations are small.

By use of the principle that the transport is directly correlated with the wind speed, and that the convergence is positive in an atmospheric "high" pressure area and negative in a "low," it is possible to discuss the annual variations which might be expected. In the trade-wind belt, the northward transport is largest in winter, but the maximum convergence comes in the early spring; while the minimum (though still large) transport and con-

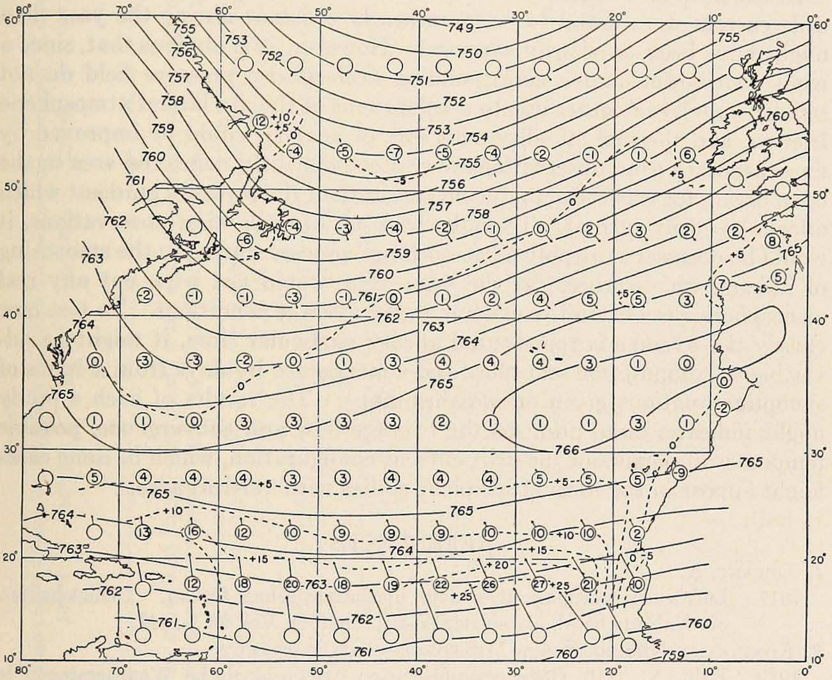

Figure 52. The solid lines are average January isobars for each mm. Hg of atmospheric pressure. The vectors represent the transport of the drift current at the center of each 5° square. The figures in circles give the convergence of the drift current in cm./day. The dotted lines connect areas of equal convergence.

vergence occur in autumn, when the pressure gradient is weakest and the isobars have the least anticyclonic curvature. Along the ridge of the Azores "high," convergence is pronounced in May and again in December, when there is a secondary maximum. In the zone of the westerlies, the greatest transport (always toward the south) occurs in late autumn and in early winter, but the convergence is largest in the spring months, although even then divergence exists east of Newfoundland. The American coastal transport is most marked in the latter part of the winter, when the maximum divergence occurs. There is little divergence in summer, when the trough of low pressure moves onto the continent. Along the African coast, divergence is most pronounced when the transport is directed as much off-shore as possible, which is the case in spring. In general, the magnitude of this divergence is directly correlated with the magnitude of the convergence in the trade-wind belt.

In conclusion, it might be stated that the characteristics of the average drift current were found to be more nearly constant during the year than might have been previously expected. However, it is obvious that, since a wind distribution and a corresponding atmospheric pressure field do not strictly match each other due to accelerations of the air, lateral atmospheric friction, and thermal stability, this sort of analysis could be improved by more accurate wind observations over a conveniently restricted area in the open ocean, for it is the actual wind rather than the pressure gradient which affects the drift current. To make best use of such wind observations, it would be necessary to apply a "smoothing" process similar to the smoothing of isobars, which process at the same time would not wipe out any real atmospheric discontinuities existing under average conditions. To test how closely the average is represented at any particular time, it might be advisable to compute the transport and convergence by days from a series of synoptic situations given on weather maps. The results of such a study might indicate, in addition to the average flow and convergence, possible temporary anomalies of the drift current configuration, which in some cases might appear in the form of incipient eddies with vertical axes.

REFERENCES

1. DEFANT, A.
1917. Luftdruckverteilung über dem nordatlantischen Ozean. Denkschriften der Kaiserliche Akademie der Wissenschaften, Vol. 93, p. 447.

2. KONINKLIJK NEDERLANDSCH METEOROLOGISCH INSTITUUT
1919. Publ. No. 110, Oceanographische en Meteorologische Waarnemingen in den Atlantischen Oceaan, Vol. for Dec., Jan., Feb. (1870–1914).

3. MONTGOMERY, R. B.
1936. Computation of the Transport of Surface Water due to the Wind System over the North Atlantic. Transactions of the American Geophysical Union, Seventeenth Annual Meeting, pp. 225–229.

4. MONTGOMERY, R. B.
1938. Circulation in Upper Layers of Southern North Atlantic Deduced with Use of Isentropic Analysis. Papers in Physical Oceanography and Meteorology, Vol. 6, No. 2, 55 pp.

5. PERLEWITZ, P.
1936. The Wind According to the Beaufort Scale and its Velocity. Hydrographic Review, Vol. 13, Part 1, p. 145.

6. ROSSBY, C.-G., AND MONTGOMERY, R. B.
1936. On The Momentum Transfer at the Sea Surface. Papers in Physical Oceanography and Meteorology, Vol. 4, No. 3, 30 pp.

TABLE I

Magnitude (tons/meter/sec) and Direction (Clockwise from N) of the Transport of the Drift Current for January

	80°–70° W.		70°–60° W.		60°–50° W.		50°–40° W.		40°–30° W.		30°–20° W.		20°–10° W.		10° W.–0°		0°–10° E.	
60° N.–50° N.					0.58 212°	0.34 197°	0.21 177°	0.21 169°	0.29 159°	0.37 148°	0.56 141°	0.67 131°	0.61 130°	0.62 132°	0.62 139°	0.53 141°	0.47 129°	0.25 124°
					0.43 214°	0.33 192°	0.35 175°	0.38 158°	0.50 148°	0.56 143°	0.61 139°	0.63 136°	0.57 134°	0.48 131°	0.39 135°	0.37 140°	0.43 140°	0.44 —
50° N.–40° N.		0.11 —	0.16 221°	0.26 209°	0.37 204°	0.32 179°	0.44 162°	0.58 155°	0.60 145°	0.65 141°	0.64 139°	0.57 138°	0.45 139°	0.35 138°	0.25 133°	0.16 130°	0.10 119°	
		0.19 218°	0.11 218°	0.08 195°	0.19 194°	0.34 162°	0.44 151°	0.50 151°	0.50 145°	0.49 139°	0.45 138°	0.34 140°	0.22 146°	0.14 145°	0.11 140°	0.09 138°		
40° N.–30° N.	0.08 217°	0.16 224°	0.14 202°	0.17 167°	0.27 161°	0.31 153°	0.34 146°	0.36 146°	0.31 139°	0.22 138°	0.12 135°	0.07 145°	— —	— —	— —			
	0.03 228°	0.09 199°	0.15 180°	0.21 153°	0.23 152°	0.20 151°	0.13 144°	0.07 137°	0.04 129°	— —	— —	— —	0.04 305°	0.05 307°	0.04 317°			
30° N.–20° N.	0.14 341°	0.08 350°	0.03 351°	— —	— —	— —	— —	0.03 343°	0.08 340°	0.12 333°	0.22 337°	0.31 331°	0.33 331°	0.23 330°				
	0.70 —	0.65 351°	0.61 352°	0.53 354°	0.57 352°	0.48 347°	0.48 342°	0.52 340°	0.45 339°	0.43 332°	0.52 327°	0.58 332°	0.65 331°					
20° N.–10° N.		1.44 —	1.52 349°	1.72 354°	1.52 352°	1.35 352°	1.21 341°	1.28 339°	1.46 341°	1.57 336°	1.65 331°	1.83 330°	2.03 331°					
			1.84 350°	2.06 359°	2.42 358°	2.37 352°	2.66 340°	3.15 337°	3.48 339°	3.49 339°	3.43 332°	3.50 323°	2.99 332°					